

Microstructure refinement and improvements of magnetic properties of  $\text{Pr}_2(\text{Fe, Co})_{14}\text{B}/\alpha\text{-(Fe, Co)}$  nanocomposites by additional Ga

This article has been downloaded from IOPscience. Please scroll down to see the full text article.

2001 J. Phys.: Condens. Matter 13 3859

(<http://iopscience.iop.org/0953-8984/13/17/306>)

View [the table of contents for this issue](#), or go to the [journal homepage](#) for more

Download details:

IP Address: 171.66.16.226

The article was downloaded on 16/05/2010 at 11:53

Please note that [terms and conditions apply](#).

# Microstructure refinement and improvements of magnetic properties of $\text{Pr}_2(\text{Fe}, \text{Co})_{14}\text{B}/\alpha\text{-(Fe, Co)}$ nanocomposites by additional Ga

Wen-Yong Zhang<sup>1</sup>, Jiang Zhang, Zhao-Hua Cheng, Shao-Ying Zhang and Bao-Gen Shen

State Key Laboratory of Magnetism, Institute of Physics and Centre of Condensed Matter Physics, Chinese Academy of Sciences, Beijing 100080, People's Republic of China

E-mail: ymjj@g203.iphy.ac.cn

Received 11 January 2001, in final form 2 March 2001

## Abstract

The effect of additive Ga on the microstructure and magnetic properties of nanocomposite  $\text{Pr}_2(\text{Fe}, \text{Co})_{14}\text{B}/\alpha\text{-(Fe, Co)}$  ribbons has been investigated. One per cent Ga addition was found to improve significantly its magnetic properties. The remanence and maximum energy product increase from 1.14 T, 17 MG Oe for Ga-free samples to 1.22 T, 22.2 MG Oe for Ga-doped samples. The significant improvements of magnetic properties originate from the refinement of the grains of the samples by introducing Ga, which leads to a stronger exchange coupling between the magnetically hard and soft phases in comparison with that in Ga-free samples.

## 1. Introduction

Nanocomposite magnetic materials consisting of a hard magnetic phase exchange coupled to a soft magnetic phase have attracted considerable interest because of their unusually high isotropic remanence ratio, high energy product and low cost [1–4]. Nanocomposite magnets have been fabricated mainly by melt spinning and mechanical alloying. Experimentally, a remanence ratio of  $M_r/M_s = 0.8$  of nanocomposite magnets, which is much higher than the Stoner–Wohlfarth limitation ( $M_r/M_s = 0.5$ ), has been achieved, but their maximum energy product (10–20 MG Oe) is still significantly lower than the theoretical prediction. This phenomenon is attributed to the difference between microstructures of the real nanocomposite magnets and the theoretical model [5–8]. The most significant difference is that the grain size obtained usually in nanocomposite magnets, 20–50 nm, is much larger than that required theoretically for getting a high maximum energy product. Although a very small grain size (10 nm) is obtained by hot compaction under high pressure, the process is time and energy consuming. Recently, it was reported that Ga addition effectively refines the grain size of

<sup>1</sup> Corresponding author.

magnetic phases in a  $\text{Nd}_2\text{Fe}_{14}\text{B}/\text{Fe}_3\text{B}$  nanocomposite [9], which strengthens the exchange coupling interaction between the magnetically hard and soft phases and finally improves the magnetic properties of nanocomposite magnets. Our recent experiments show that the substitution of Co for Fe improves greatly the saturation magnetization of  $\text{Pr}_2\text{Fe}_{14}\text{B}/\alpha - \text{Fe}$  nanocomposites, however, and also leads to a coarse grain size [10]. In this paper, we present a study of the effects of Ga addition on the microstructure and magnetic properties of  $\text{Pr}_2(\text{Fe}, \text{Co})_{14}\text{B}/\alpha - (\text{Fe}, \text{Co})$  nanocomposites.

## 2. Experiment

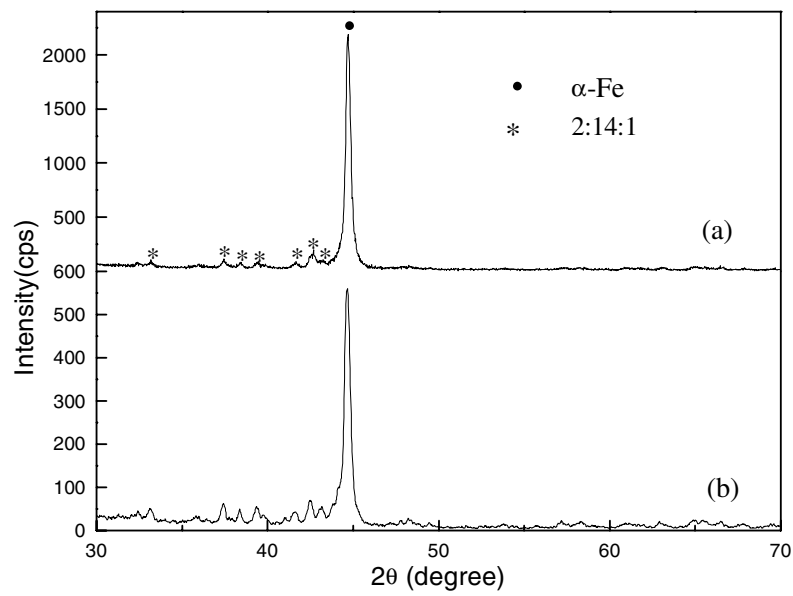
The master alloys of  $\text{Pr}_9\text{Fe}_{74}\text{Co}_{12}\text{B}_5$  and  $\text{Pr}_9\text{Fe}_{74}\text{Co}_{12}\text{GaB}_5$  were prepared by arc melting under argon atmosphere from the constituent elements Pr, Fe, Co, Ga (purity  $\geq 99.9\%$ ) and an FeB pre-alloy. The ribbons with 1 mm width and 40  $\mu\text{m}$  thickness were obtained using the melt-spinning technique in an argon atmosphere. The surface velocity of the Cu wheel ranges from 6 to 40  $\text{m s}^{-1}$ .

X-ray diffraction (XRD) with Cu  $K\alpha$  radiation was used to identify the phase composition of the sample. An H-800 transmission electron microscope (TEM) was employed to observe the microstructure of the sample. The Curie temperatures ( $T_C$ ) of magnetic phases in the ribbons were determined by the measurements of the temperature dependence of magnetization at a temperature ranging from the room temperature to 1273 K in a field of 1 kOe. The magnetic properties of the samples were measured with a superconducting quantum interference device (SQUID) magnetometer using an applied field of 5 T. The applied field is parallel to the longitudinal axis of the ribbons.

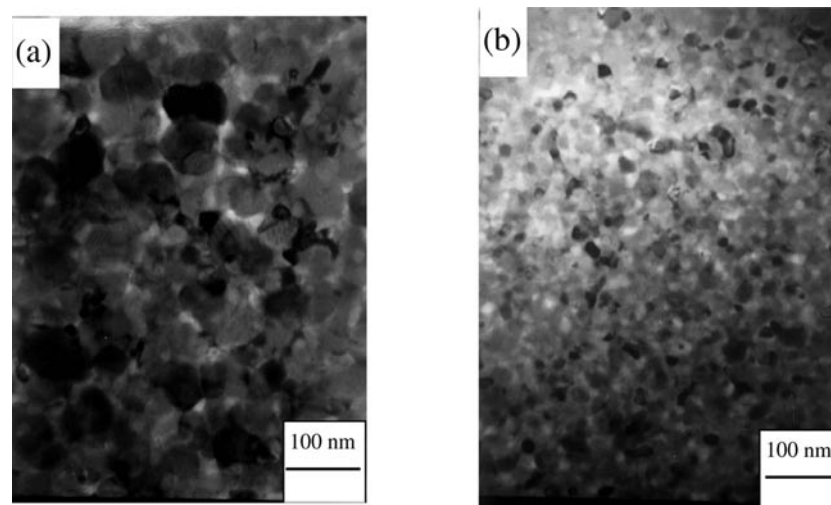
## 3. Results and discussion

Figure 1 shows the XRD patterns of Ga-free and Ga-doped ribbons spun at the optimum wheel speed of 17.5  $\text{m s}^{-1}$  where the maximum coercivity was obtained. It is found that the ribbons consist of the hard magnetic 2:14:1 phase and soft magnetic  $\alpha - (\text{Fe}, \text{Co})$  phase. No obviously preferential orientation of the crystallites is observed from the diffraction peaks. Therefore, it may be inferred that the structure is isotropic. The (110) diffraction peak of  $\alpha - (\text{Fe}, \text{Co})$  remains at  $2\theta = 44.68^\circ$ , which implies that the Ga atom does not dissolve in the  $\alpha - (\text{Fe}, \text{Co})$  to form (Fe,Co)Ga dilute alloys. One may notice that the diffraction peaks of the 2:14:1 and  $\alpha - (\text{Fe}, \text{Co})$  phases in the Ga-doped ribbons are obviously broadened in comparison with that in the Ga-free ribbons, which implies that Ga addition leads to the decrease of the grain size. Using the Scherrer formula, it is estimated that the average grain sizes of the 2:14:1 in Ga-free and Ga-doped ribbons are 40 nm and 20 nm, respectively, and the mean grain sizes of the  $\alpha - (\text{Fe}, \text{Co})$  phase in Ga-free and Ga-doped ribbons are 40 nm and 15 nm, respectively. This further demonstrates that Ga addition refines grains of the samples. In addition, no new phase seems to be present after the addition of Ga from the XRD graphs in figure 1.

Figure 2 presents two TEM micrographs of grain morphology of the ribbons: (a) shows abnormally coarse  $\alpha - (\text{Fe}, \text{Co})$  with a mean grain size of about 40 nm for Ga-free ribbons; (b) shows a uniform distribution of fine grains with mean grain size of about 15 nm for Ga-doped ribbons. It is obvious that Ga addition is effective for reducing the grain size of the samples. The TEM observations agree well with the results calculated from XRD patterns. We know that the substitution of Ga for Fe will result in the change of  $T_C$  of 2:14:1 for  $\text{Pr}_2\text{Fe}_{14-x}\text{Ga}_x\text{B}$  systems [11]. Our thermomagnetic measurements show that the Curie temperature 668 K of 2:14:1 in Ga-free ribbons is almost the same as that 669 K in Ga-doped ribbons. So it is



**Figure 1.** XRD patterns of Ga-free (a) and Ga-doped (b) ribbons spun at the optimum wheel speed of  $17.5 \text{ m s}^{-1}$ .



**Figure 2.** TEM micrographs of grain morphology of the ribbons spun at the optimum wheel speed of  $17.5 \text{ m s}^{-1}$ : Ga-free ribbons (a) and Ga-doped ribbons (b).

concluded that the Ga atom enriches the grain boundary, which is believed to act as a grain growth inhibitor of the  $\alpha$ -(Fe, Co) and 2:14:1 phases and leads to the formation of ultrafine grain structure. Similar results are observed in a  $\text{Nd}_2\text{Fe}_{14}\text{B}/\text{Fe}_3\text{B}$  nanocomposite [9].

Figure 3 illustrates the room-temperature demagnetization curve of Ga-free and Ga-doped ribbons spun at the optimum wheel speed of  $17.5 \text{ m s}^{-1}$ . The remanence and intrinsic coercivity increase from 1.14 T and 5.9 kOe for the Ga-free sample to 1.22 T and 6.3 kOe

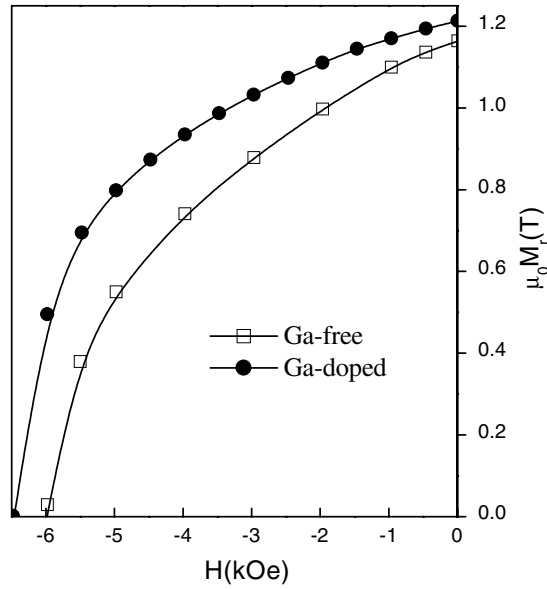


**Figure 3.** Room temperature demagnetization curve of Ga-free and Ga-doped ribbons spun at the optimum wheel speed of  $17.5 \text{ m s}^{-1}$ .

for the Ga-containing one, respectively. Furthermore, the introduction of Ga leads to a more convex demagnetization curve. Owing to its higher remanence and better rectangularity of demagnetization curve, the maximum energy product of the Ga-containing sample increases by about 30% from 17 MG Oe to 22.2 MG Oe compared with that of the Ga-free one.

For Ga-free and Ga-doped ribbons spun at the optimum wheel speed of  $17.5 \text{ m s}^{-1}$ , the temperature dependence of  $iH_c$  and  $M_r$  is shown in figure 4. It can be found that  $iH_c$  rapidly increases while the remanence slightly increases with the temperature decreasing from RT to 150 K. Within the whole temperature range, the  $M_r$  for the Ga-doped sample is higher than that for the Ga-free sample, which indirectly illuminates that the exchange-coupling interaction between the magnetically hard/soft phase in the Ga-doped sample is stronger than that in the Ga-free sample. The similar phenomenon is found in the Cu-free and Cu-doped  $\text{Sm}_2\text{Fe}_{14}\text{Si}_2\text{C}$  ribbons [12].

To obtain quantitative information about the effect of Ga addition on the microstructure of the ribbons, we analyse the temperature dependence of  $\mu_{0i}H_c$  in the framework of the nucleation model using a modified form of Brown's expression for the nucleation field of an ideal homogeneously magnetized particle [13–18]:

$$\mu_{0i}H_c(T) = \alpha_k \alpha_{ex} \mu_0 H_N^{min}(T) - N_{eff} J_s(T) \quad (1)$$

where the microstructural parameters  $\alpha_k$ ,  $\alpha_{ex}$  and  $N_{eff}$  are related to the non-ideal microstructure of the real magnet:  $\alpha_k$  describes the influence of the non-perfect surface of the grains on the crystal anisotropy.  $N_{eff}$  is the effective demagnetization factor describing the internal stray fields acting on the grains.  $\alpha_{ex}$  takes into account the effect of the exchange coupling between neighbouring grains.  $\mu_0 H_N^{min} = (K_1 + 2K_2)/J_s$ . In the case of vanishing  $K_2$  values,  $\mu_0 H_N^{min} = K_1/J_s$ . To calculate the values,  $\mu_0 H_N^{min}(T)$ , we used the intrinsic magnetic properties  $J_s(T)$  and  $K_1(T)$  from measurements made with a  $\text{Pr}_2\text{Fe}_{14}\text{B}$  single crystal [19]. From the temperature dependence of the coercive field, the microstructural parameters  $\alpha_k \alpha_{ex}$  and  $N_{eff}$  according to equation (1) can be determined by plotting the experimental

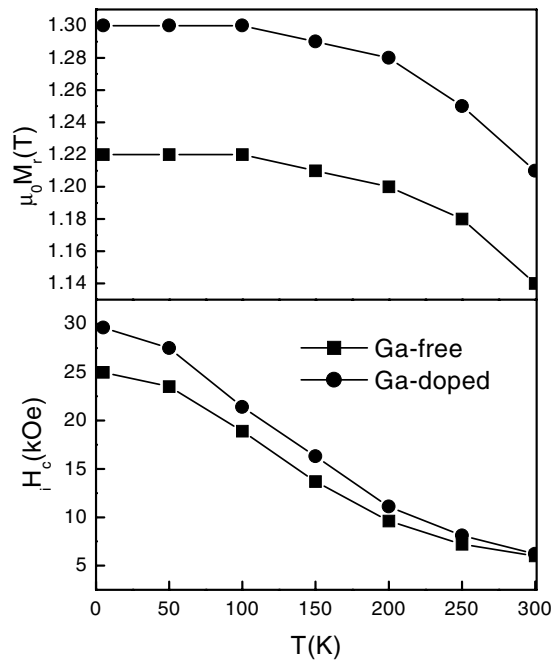


**Figure 4.** Temperature dependence of coercivity  $H_c$  and remanence  $M_r$  for Ga-free and Ga-doped ribbons spun at the optimum wheel speed of  $17.5 \text{ m s}^{-1}$ .

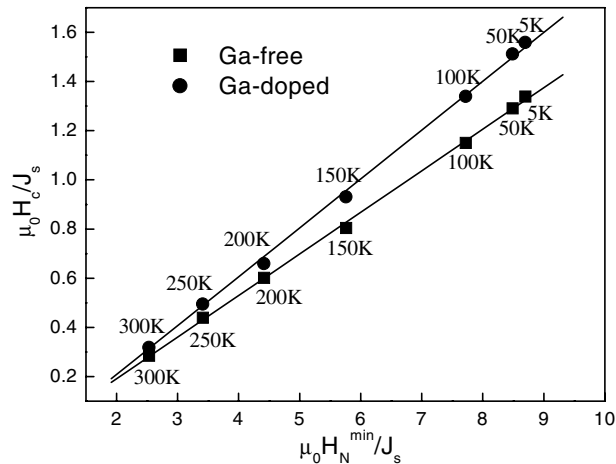


**Figure 5.**  $\mu_0 H_c / J_s$  versus  $\mu_0 H_N^{min} / J_s$  for Ga-free and Ga-doped ribbons spun at the optimum wheel speed of  $17.5 \text{ m s}^{-1}$ .

data  $\mu_0 H_c / J_s$  versus the theoretical values  $\mu_0 H_N^{min} / J_s$ . This evaluation is shown in figure 5. A linear relation is found in the whole temperature range. As the parameter  $\alpha_k$  varies in the range  $0.7 < \alpha_k < 0.9$  [18, 20], to compute the absolute values of  $\alpha_{ex}$  of the exchange coupled magnets, we assume  $\alpha_k = 0.8$ . For the Ga-free sample,  $\alpha_{ex}$  and  $N_{eff}$  is 0.20 and 0.12, respectively. For the Ga-containing sample,  $\alpha_{ex}$  and  $N_{eff}$  is 0.25 and 0.19, respectively. The larger value of  $\alpha_{ex}$  indicates that the exchange-coupling interaction between the 2:14:1

and  $\alpha$ -(Fe, Co) for the Ga-containing sample is stronger than that for the Ga-free sample. According to micromagnetic calculations [21], this enhancement of the coupling behaviour arises from the grain refinement of  $\alpha$ -(Fe, Co) due to Ga addition (see figure 2). The closer the grain size of soft magnetic phase is to twice the domain wall width of the hard magnetic phase, the stronger the exchange coupling interaction between grains is. In the Ga-doped ribbons, the value of  $N_{eff}$  is one and a half times as large as that in Ga-free ribbon; a possible reason is that the partial grains in Ga-doped are separated from each other by nonmagnetic Ga-rich phase at the grain boundary.

#### 4. Conclusion

We have reported a strong influence of Ga addition on microstructures and magnetic properties of the  $\text{Pr}_9\text{Fe}_{74}\text{Co}_{12}\text{B}_5$  ribbon. The introduction of Ga refines the grains of the magnetic phases, which results in a stronger exchange coupling between the magnetically hard/soft phase compared with that in Ga-free ribbon. The remanence and the maximum energy product increase from 1.14 T, 17 MG Oe for Ga-free samples to 1.22 T, 22.2 MG Oe for Ga-doped samples. The temperature dependence of coercive field quantitatively demonstrates that Ga addition enhances the exchange coupling interaction between the magnetically hard/soft phases.

#### Acknowledgments

This work was supported by the State Key Project of Fundamental Research and the National Natural Science Foundation of China. The authors wish to express their gratitude to T S Ning and M Hu for their assistance in performing magnetic measurements.

#### References

- [1] Kneller E F and Hawig R 1991 *IEEE Trans. Magn.* **27** 3588
- [2] Skomsi R and Coey J M D 1993 *Phys. Rev. B* **48** 15 812
- [3] Schrefl T, Kronmüller H and Fidler J 1993 *J. Magn. Magn. Mater.* **27** L273
- [4] Panagiotopoulos I, Withanawasam L, Murthy A S and Hadjipanayis G C 1996 *J. Appl. Phys.* **79** 4827
- [5] Ding J, McCormick P G and Street R 1993 *J. Magn. Magn. Mater.* **124** 1
- [6] Withanawasam L, Murthy A S and Hadjipanayis G C 1995 *IEEE Trans. Magn.* **31** 3608
- [7] Chang W C, Chiou D Y and Wu S H 1998 *Appl. Phys. Lett.* **72** 121
- [8] McCormick P G, Miao W F, Smith P A I, Ding J and Street R 1998 *J. Appl. Phys.* **83** 6256
- [9] Ping D H, Hono K and Hirotsawa S 1998 *J. Appl. Phys.* **83** 7769
- [10] Zhang W Y, Yan A R, Zhang H W and Shen B G 2001 *J. Alloys Compounds* **315** 174
- [11] Pedziwiatr A T, Sankar S G and Wallace W E 1988 *J. Appl. Phys.* **63** 3710
- [12] Zhang H W, Zhang S Y and Shen B G 1998 *J. Appl. Phys.* **83** 4838
- [13] Bauer J, Seeger M, Zern A and Kronmüller H 1996 *J. Appl. Phys.* **80** 1667
- [14] Kronmüller H 1987 *Phys. Status Solidi b* **144** 385
- [15] Kronmüller H, Durst K D and Sagawa M 1988 *J. Magn. Magn. Mater.* **74** 291
- [16] Martinek G and Kronmüller H 1990 *J. Magn. Magn. Mater.* **86** 177
- [17] Kronmüller H 1991 *Supermagnets* ed G J Long and F Grandjean (Dordrecht: Kluwer) p 1461
- [18] Seeger M, Köhler D and Kronmüller H 1994 *J. Magn. Magn. Mater.* **130** 165
- [19] Hirotsawa S, Matsuura Y, Yamamoto H, Fujimura S, Sagawa M and Yamauchi H 1986 *J. Appl. Phys.* **59** 873
- [20] Köhler D 1992 *Thesis* University Stuttgart
- [21] Schrefl T, Fidler J and Kronmüller H 1994 *Phys. Rev. B* **49** 6100